

7 - Summary of Results

INTRODUCTION

In this final chapter of the Initial Report, the major geological outcomes of CRP-2/2A are summarised, conclusions are drawn and plans for the final drilling season are set out. Although the Initial Report as a document is focussed primarily on core characterization, a number of important conclusions can already be drawn from the geological and geophysical analyses carried out during and immediately following the drilling season at Cape Roberts and McMurdo Station. This chapter contains four substantive sections, which deal with the major outcomes of CRP-2/2A in terms of geochronology, climatic and depositional history, and volcanic-tectonic history, followed by some conclusions and plans for the future.

Current chronological interpretations of the strata penetrated by CRP-2/2A are based on biostratigraphy (principally utilising marine diatoms and, to a lesser extent, calcareous nannofossils), palaeomagnetic studies and $^{40}\text{Ar}/^{39}\text{Ar}$ dates from the volcanic tephra unit at 109-114 mbsf. The distribution of microfossils recovered from the core is irregular. This, together with the abundance of coarse-grained lithologies, the numerous disconformities recorded in the core, and variable palaeoenvironmental conditions, have complicated interpretation of the distribution of key fossil taxa in CRP-2/2A. In addition, some microfossil groups are either previously undescribed or are known to be endemic to the region, further frustrating efforts to compile an integrated biostratigraphical framework for the hole.

The initial magnetic polarity stratigraphy for CRP-2/2A is divided into 14 magnetozones, of which 12 are pre-Pliocene in age. Several key diatoms and nannofossils, together with the $^{40}\text{Ar}/^{39}\text{Ar}$ age determination at 113 mbsf (21.44 ± 0.05 Ma), constrain correlation of these magnetozones to the magnetic polarity time scale, allowing construction of a preliminary, integrated age-depth plot. The current interpretation for the cored succession places Quaternary strata from the sea floor to 21.20 mbsf, a thin Pliocene interval from 21.20 to 26.80 mbsf, early Miocene strata from 26.80 to 130.27 mbsf, late Oligocene strata from 130.27 to 306.65 mbsf, and early Oligocene (with possibly some latest Eocene) strata from 306.65 mbsf to the base of the hole at 624.15 mbsf.

On the basis of the facies analysis reported in chapter 3, the core has been interpreted in terms of an array of glacial-marine and open coastal/shelf depositional environments, involving repeated advance and retreat of floating and grounded ice across the shelf. The facies assemblage is considered to be typical of cool, but not cold, climate, polythermal glaciers with considerable melt-water discharge in the Oligocene, but with less melt-water

influence in the Miocene. Palynological investigations also suggest that, even in the oldest strata recovered from CRP-2/2A, climatic conditions were not fully temperate.

The abundant and extensive deformational features preserved in the core may partially reflect glacial over-riding of the drill-site at various times. If subglacial over-riding and deposition is recorded in the core, the glaciers responsible were probably grounded on the continental shelf. Twenty-four vertically stacked, erosionally-based, cyclic facies successions (sequences) are interpreted as recording cycles of glacier advance and retreat across the area, and broad variations in shelfal water depths of the order of 50-100 m. The uppermost two sequences are amalgamated, recording a cryptic and incomplete Quaternary and Pliocene record that accumulated during a period of low net accommodation. The early Miocene and Oligocene record, on the other hand, is relatively more complete with 6 and 16 sequences, respectively, recognized. The controlling factors on this cyclicity cannot yet be fully evaluated.

Sediments preserved in CRP-2/2A were derived from a variety of rock types, all of which crop out in the area landward of Cape Roberts, suggesting a relatively local provenance. A major change in sediment provenance is recorded in the core at about 310 mbsf (close to the preferred location for a Late/Early Oligocene unconformity), from detritus derived predominantly from Jurassic dolerites, lavas and Beacon Supergroup sedimentary rocks, to detritus containing additional abundant basement granitoid material. Up-hole changes in the relative abundances of different extraformational sediment types are interpreted as recording the progressive unroofing of the Transantarctic Mountains. This may have been a consequence of earlier, or continuing, uplift in a period when climate was warmer and allowed greater amounts of fluvial sediment transport than at present.

Superimposed on this pattern is a contemporaneous record of volcanic activity. Petrographical evidence suggests that volcanic activity associated with the McMurdo Volcanic Group was active as far back as the Early Oligocene, which confirms a longer history of McMurdo Volcanic Group activity than that known from onshore. The sources for this volcanic material, including a spectacular, tephra-rich interval dated as early Miocene in age, may have been local to the Cape Roberts area, though the possibility of a more distant source remains.

The implications of CRP-2/2A for basin history cannot yet be fully assessed. Cyclical variation in the thickness of depositional sequences may indicate changes in subsidence regime through time, and the extensive deformation preserved in the core may in part record tectonic activity. Furthermore, initial correlation of the core with seismic

records and the near doubling of sonic velocity of strata below 300 mbsf indicate that tectonic dips are twice that which had been inferred previously (Barrett et al., 1995; Bartek et al., 1996). Dips are interpreted as increasing with depth, and truncations indicate angular discordances. Such features may be related to discrete episodes of rifting associated with the evolution of the Victoria Land Basin. Testing of these ideas must await further research.

CHRONOLOGY

The biostratigraphical framework for the pre-Pliocene section of CRP-2/2A is provided primarily by marine diatoms and, to a lesser extent, by calcareous nannofossils. There is considerable variation in distribution and abundance of these microfossils throughout the core (see chapter 5) and representation by open-ocean pelagic diatom or nannofossil taxa, which provide direct correlations to Southern Ocean and global bio- and chronostratigraphies, is limited.

As in CRP-1 (Harwood et al., 1998), marine diatoms are the most abundant and age-diagnostic forms recovered in CRP-2/2A. The diatom floras constrain the age of several intervals of CRP-2/2A by comparison with Southern Ocean Deep Sea Drilling Project (DSDP) and Ocean Drilling Program (ODP) drill holes. Assemblages are compared, for correlation purposes, with the CIROS-1, MSSTS-1, and CRP-1 cores from the Ross Sea. Calcareous nannofossils also provide important constraints on the age of CRP-2/2A by correlation to DSDP and ODP drill holes, and to CIROS-1. Foraminifera and marine palynomorphs have biostratigraphical potential. However, the foraminifera found in the core are all benthic forms; planktic age-diagnostic taxa are entirely absent. Marine palynomorphs (dinoflagellate cysts and acritarchs) are abundant and varied, but the floras are endemic, with many new species, and cannot currently provide biostratigraphical control for the Miocene and Oligocene. Radiometric dates ($^{40}\text{Ar}/^{39}\text{Ar}$) on two volcanic ash layers,

together with magnetostratigraphy, provide additional chronological constraints. Seven pre-Pliocene magnetozones are defined above 350 mbsf (N2 to the upper part of N5; Fig. 7.1). Below 350 mbsf, 6 magnetozones are defined (the lower part of N5 to R7). These lower magnetozones are poorly defined and further analyses are necessary to improve the magnetostratigraphy. A preliminary age-depth plot and correlation to the magnetic polarity timescale (MPTS) is presented in figure 7.1. The correlation is discussed below.

Sporadic fossil occurrences, coarse lithofacies, numerous disconformities and variable palaeo-environmental conditions all make it difficult to establish the complete distribution of key fossils in the pre-Pliocene interval of CRP-2/2A (26.75-624.15 mbsf). There are numerous stratigraphical breaks (disconformities) that divide the CRP-2/2A record into discrete packages of strata. The most significant breaks occur at three of the major sequence boundaries: *c.* 130, 307 and 443 mbsf (see chapter 3). These disconformities define four stratigraphical intervals, which are discussed below.

The uppermost interval, from 26.75 to *c.* 130 mbsf, is geochronologically well constrained by the first common occurrence of *Thalassiosira praeфрага* at 36.25 mbsf (D3; Tab. 7.1 and Fig. 7.1), which ranges from the upper part of Chron C6r through Chron C6n (Gersonde & Burckle, 1990; Baldauf & Barron, 1991; Harwood & Maruyama, 1992). In CRP-2/2A, this datum occurs near the base of a normal polarity interval (magnetozone N2) that we correlate with Chron C6n. The interval from 36.25 to *c.* 130 mbsf is confined to the middle lower Miocene by a volcanic ash at *c.* 113 mbsf that is dated at 21.44 ± 0.05 Ma by the $^{40}\text{Ar}/^{39}\text{Ar}$ method (A9 in Fig. 7.1). Chron C6Ar (21.32-21.77 Ma; Cande & Kent, 1995; Berggren et al., 1995) spans the age of the ash (including the uncertainty on the age determination). The ash, however, lies within a thick normal polarity magnetozone (N3, 71.89-127.70 mbsf; Fig. 7.1). It is unlikely that the ash was reworked significantly (see Volcanic Clasts section). Our preferred explanation for this discrepancy is that, given uncertainties

Tab. 7.1 - Biostratigraphical datum events in CRP-2/2A.

Event	Datum	CRP-2/2A Depth (mbsf)	Age (Ma) / Chron
D3	FO <i>Thalassiosira praeфрага</i> complex [†]	36.25	20.3 (C6r)
D7	FO <i>Dactyliosolen antarcticus</i>	75.56	26.5 (C8n.2n)
D8	FO <i>Asteromphalus symmetricus</i>	236.25*	28.7 (C10n.2n)
D9	LO <i>Lisitzinia ornata</i> [‡]	259.21	24.2 (C6Cr)
D10	FO <i>Lisitzinia ornata</i> [‡]	266.38	28.2 (C9r)
D11	FO <i>Cavitatus jouseanus</i>	292.09*	30.9 (C12n)
D12	LO <i>Asterolampra punctifera</i>	444.96**	27.0 (C9n)
D13	LO <i>Pyxilla reticulata</i>	444.96**	30.1 (C11r)
D14	LO <i>Rhizosolenia oligocaenica</i>	444.96**	31.0 (C12r)
D15	FO <i>Rhizosolenia oligocaenica</i>	483.96*	33.5 (C13n) or older?
N1	LO <i>Dictyococcites bisectus</i>	144.44	23.9 (C6Cn.2r)
N2	LO <i>Isthmolithus recurvus</i>	459.52	31.8 (C12r)
N3	LO <i>Reticulofenestra oamaruensis</i>	458.40	33.7 (C13r)
A9	Ash	111.58 to 114.15	21.44 ± 0.05
A10	Ash	280.03 to 280.12	24.22 ± 0.06

Note: * = lowest confirmed occurrence in CRP-2/2A; ** = highest confirmed occurrence in CRP-2/2A;

† = age-depth interpretations of CRP-1 place datum in C6r to C5En (Roberts et al., 1998); ‡ = total range of taxon is most likely more restricted on Antarctic shelf than in deep-sea.

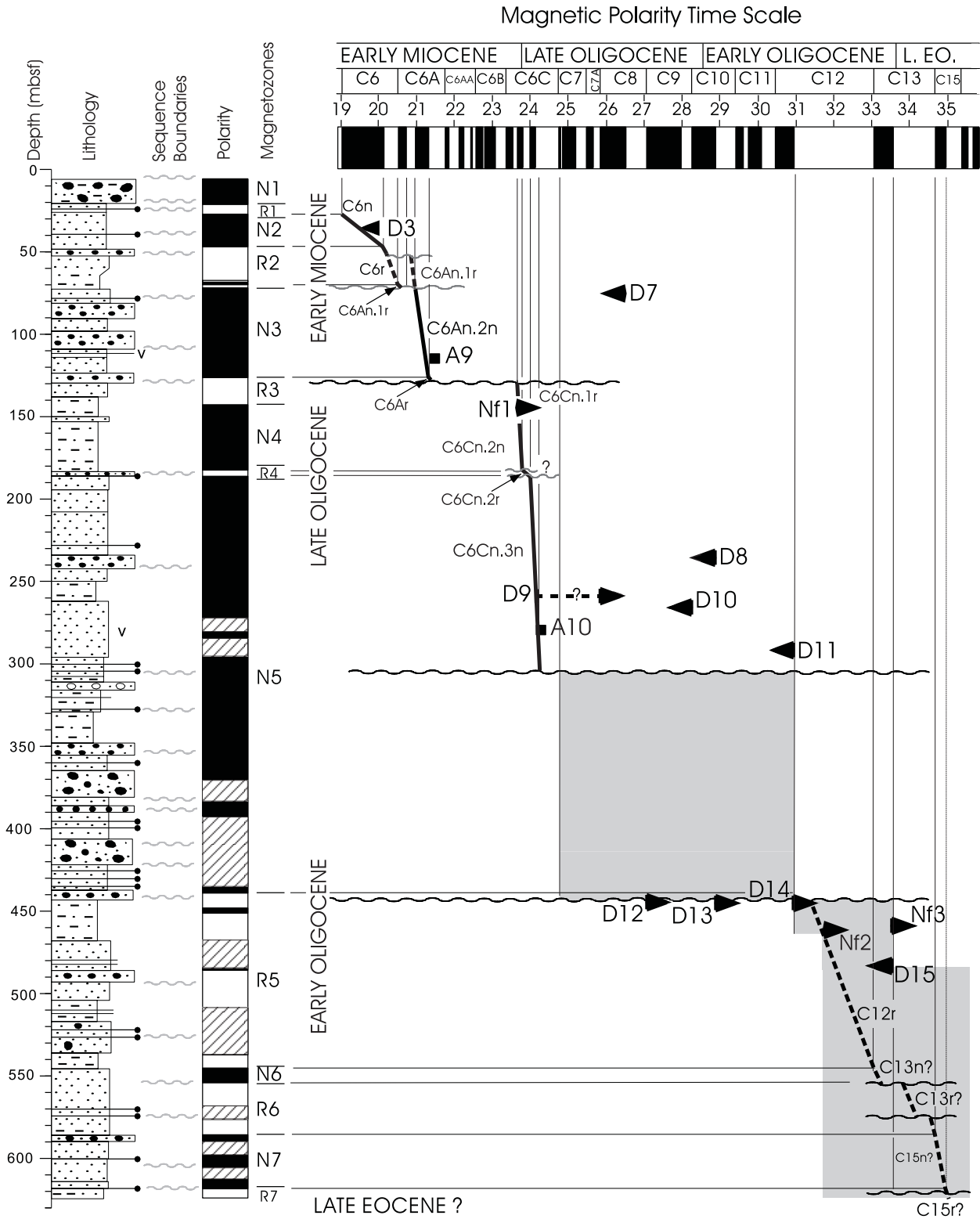


Fig. 7.1 - Correlation of CRP-2/2A with the MPTS of Cande & Kent (1995) and Berggren et al. (1995) using the preliminary magnetic polarity zonation (black = normal polarity, white = reversed polarity, hatched = unresolved) defined in chapter 6 (Palaeomagnetism), palaeontological datum events (chapter 5), and two radiometric ages described in chapter 4 (Volcanic Clasts section) and in the note following this section. The tip of the arrow marking each datum indicates its stratigraphical position and the base of the arrow is aligned with its age on the MPTS. Major unconformities are defined both by lithological sequence boundaries (see chapter 3, Sequence Stratigraphical Interpretation section) and by palaeontological datums. Other unconformities that coincide with lithostratigraphical breaks (see chapter 3, Description of Sequence section) are defined by the magnetic polarity stratigraphy (see chapter 6). Palaeontological and radiometric datums are defined in table 7.1. The datums are numbered according to the designations given by Roberts et al. (1998): diatom datums not reported in CRP-1 are given higher numbers, starting with D7. The shaded area below 307 mbsf defines the envelope of other possible correlations that are consistent with the data. Stepwise appearances are defined by the datums and do not imply the presence of additional disconformities in the sequence. A tentative interpretation is presented for the interval below 443 mbsf.

in numerical ages assigned to $^{40}\text{Ar}/^{39}\text{Ar}$ standards (Renne et al., 1998) and uncertainties in calibration of the MPTS in the early Miocene, the ash actually fell within the nearest normal polarity chron (C6An.2n). We correlate the thin reversed polarity interval directly above magnetozone N3 with C6An.1r. In this interpretation, magnetozone N3 is truncated by an inferred disconformity (at *c.* 70 mbsf) in which we interpret little time as having been lost. The normal polarity zone below the ash bed (*c.* 113 mbsf) is interpreted as part of C6An.2n and the transition from reversed to normal polarity (magnetozone R3 to N3) immediately above the disconformity at *c.* 130 mbsf is interpreted as representing the boundary between Chrons C6Ar and C6An.2n (middle early Miocene). There is no independent evidence for the inferred disconformity at *c.* 70 mbsf (which occurs in a high-stand systems tract) and a second interpretation is possible in this interval. In this interpretation, there is no time missing in a disconformity at *c.* 70 mbsf, magnetozone R2 would represent Chron C6An.1r, and the single normal polarity sample at the base of magnetozone R2 would have no correlative in the MPTS. The sequence boundary at *c.* 52 mbsf would therefore represent a disconformity (with *c.* 500 kyr missing) and the polarity transition from Chron C6r to C6n would lie immediately above the disconformity. This second interpretation only differs from the first interpretation in the interval between 52 and *c.* 70 mbsf (Fig. 7.1). At this stage, we cannot discriminate between these two possible interpretations.

A second stratigraphical interval is defined by the disconformities at *c.* 130 and 307 mbsf. There is a major change in the diatom flora at *c.* 130 mbsf, but poor age calibration prevents direct assessment of the hiatus. However, the calcareous nannofossil assemblage that accompanies *Dictyococcites bisectus* at 144.44 mbsf (Nf1, 23.9 Ma; Tab. 7.1 and Fig. 7.1) and an $^{40}\text{Ar}/^{39}\text{Ar}$ date on a second ash layer (A10; Fig. 7.1) at 280 mbsf (24.22 ± 0.06 Ma) suggest a hiatus of at least 2 m.y. at 130 mbsf. Normal polarity is dominant between 143.90 and *c.* 307 mbsf. A sequence stratigraphical boundary at *c.* 188 mbsf marks the base of a thin interval of reversed polarity (magnetozone R4) which separates magnetozones N4 and N5 (Fig. 7.1). Given these constraints, it is most likely that the interval defined by the lower part of magnetozone R3, and by magnetozones N4, R4, and the upper part of N5 correlate with C6Cn.1r, C6Cn.2n, C6Cn.2r, and C6Cn.3n, respectively. The ash itself should lie within Chron C6Cr, but given the same level of chronological uncertainty as explained for the ash at *c.* 113 mbsf, the apparently rapid sedimentation (*c.* 300 m/My), and the lack of physical evidence for a hiatus, it is more likely that the ash occurs within the lower part of C6Cn.3n. This correlation is broadly consistent with the biostratigraphical datums. There is a slight discrepancy with the range of the diatom *Lisitzinia ornata* (D9-D10, 259.21-266.4 mbsf, 24.2-28.2 Ma). In addition, a biostratigraphical break is recognized between *c.* 266 and 271 mbsf, where the ranges of six taxa are truncated, which suggests that the base of the range of *L. ornata* may be truncated. This palaeontologically defined break was not recognized during

lithological description and is not shown in the correlation discussed above (Fig. 7.1). Further work is needed to understand these discrepancies, but, based on the above chronological interpretation, it seems unlikely that this break represents a significant hiatus.

The third disconformity-bounded interval (*c.* 307 to 443 mbsf) is poorly defined on the basis of biostratigraphy. Throughout most of its thickness (*c.* 314 to 411 mbsf), this interval is devoid of age-diagnostic siliceous or calcareous microfossil assemblages. Normal polarity is dominant in the upper part of the interval, which must therefore correlate with C7n or with older periods of normal polarity. This suggests that at least Chron C6Cr (24.12-24.73 Ma) was lost in the hiatus at *c.* 307 mbsf. The lower Oligocene diatom assemblages from *c.* 412 through 443 mbsf contain neither *Cavitatus jouseanus* nor *Rhizosolenia oligocaenica*. This suggests that the age of the base of the interval is younger than 31 Ma, and that the base of magnetozone N5 could lie within C12n (Fig. 7.1). However, palaeoecological exclusion of either taxon is possible and there are indications that the disconformity at *c.* 443 mbsf is significant (*i.e.* the biostratigraphical ranges of nine diatom taxa are truncated at this horizon). In addition, the interval between *c.* 307 and 412 mbsf contains several possible unconformities (see chapter 3, Sequence Stratigraphical Interpretation section), and time may be distributed through several normal subchrons (C7n-C12n) in this interval. The uncertainty in chronological interpretation of this interval is indicated by the shading on figure 7.1.

The lowermost stratigraphical interval (*c.* 443 to 624.15 mbsf) is biostratigraphically well constrained only in the upper 40 m. The presence of *R. oligocaenica* indicates an age of between 31.0 and 33.5 Ma. A single specimen of the calcareous nannofossil *Isthmolithus recurvus* (at 459.52 mbsf) is consistent with this age assignment (Nf2, Tab. 7.1, Fig. 7.1), which suggests correlation of magnetozone R5 with Chron C12r. However, the calcareous nannofossil *Reticulofenestra oamaruensis* occurs up to 458.12 mbsf (Nf3; Tab. 7.1 and Fig. 7.1). The LO of *R. oamaruensis* is well documented in C13r (Berggren et al., 1995), and not C12r, as shown on the preliminary correlation in figure 7.1. It is possible that *R. oamaruensis* reworked in CRP-2/2A because other floral and faunal evidence suggests that this interval is of early Oligocene age (see Palaeontology chapter). An increased abundance of reworked Eocene dinoflagellate cysts between *c.* 437 and 475 mbsf (see chapter 5, Palynology section) supports this possibility.

The *c.* 50 m interval below 484 mbsf is barren of age-diagnostic siliceous or calcareous microfossils. Taxa that are not age-diagnostic are found in intervals from *c.* 544 to 565 mbsf and from *c.* 565 mbsf to the bottom of the hole (624 mbsf). Microfossils are poorly preserved in the lowermost interval. A similar interval of poor siliceous microfossil preservation was recovered below 500 mbsf in CIROS-1. The absence of the diatom *Distephanosira architecturalis*, a widespread Southern Ocean taxon with a well-calibrated LO at 36.5 Ma (Harwood & Maruyama, 1992), suggests a likely maximum age for this interval. This absence, however, may be a purely diagenetic phenomenon.

Correlation of magnetozones N6, R6, N7, and R7 to the MPTS is ambiguous. Microfossil evidence suggests that the base of the hole is no older than latest Eocene in age (also, see note below on recognition of the Eocene-Oligocene boundary). The magnetic polarity zonation at the base of CRP-2/2A is uncertain. However, the biostratigraphical constraints, in conjunction with the presence of considerable thicknesses of reversed polarity, suggest that the base of the hole may range in age between Chron C13r and C15r (c. 33.5-35 Ma). A tentative correlation, which will be tested by further work, is shown (Fig. 7.1).

The above-described age model implies that the pre-Pliocene portion of CRP-2/2A spans an interval of 14-16 m.y. from the early Miocene (19 Ma) at 27 mbsf to the early Oligocene (or possibly latest Eocene, 33.5-35 Ma) at the base (624.15 mbsf). The age model is well defined down to 307 mbsf (c. 24 Ma), and indicates sediment accumulation rates that range between 30 and 300 m/My, with a 2 My hiatus at c. 130 mbsf. Below 307 mbsf, the age model is poorly constrained, although a significant time break is inferred at 443 mbsf, as suggested by the truncation of several diatom datums.

RECOGNITION OF THE EOCENE-OLIGOCENE BOUNDARY

A key issue for the lowermost part of CRP-2/2A is the question of what constitutes a late Eocene assemblage. The faunally and floristically rich assemblages which characterize all major groups of marine microfossils and the terrestrial palynomorphs in the Eocene do not extend to the very end of the epoch, as currently defined by Berggren et al. (1995). This is, in part, a result of repositioning of the boundary at a later level by those authors, and it also reflects a major environmental and biotic turnover that began before the end of the Eocene, as previously defined. The Antarctic floras and faunas that are preserved tend to be highly endemic, specialized polar associations, and they are often restricted to currently non-diagnostic benthic and regional neritic biotas (see chapter 5). The degree of possible diachroneity in first or last appearances for many of the Antarctic fossil taxa is still uncertain. Thus, unambiguous recognition of the Eocene is problematical, especially given the apparent lack of incursions of global oceanic waters during the time represented by the basal part of the core and the resulting lack of global ocean microfossil assemblages.

⁴⁰Ar/³⁹Ar AGE FOR PUMICE AT 280 MBSF (NOTE ADDED IN PROOF)

Feldspar crystals from a pumice-rich layer at 280 mbsf in CRP-2A provide a precise ⁴⁰Ar/³⁹Ar age of 24.22 ± 0.06 Ma. A total of fifty-five 1 to 2 mm diameter potassium-feldspar phenocrysts were extracted from pumice lapilli sampled from a pumice concentration zone near 280 m in CRP-2A. Following neutron irradiation at Texas A & M Nuclear Science Center, samples were analyzed by the ⁴⁰Ar/³⁹Ar single-crystal laser fusion method in the New

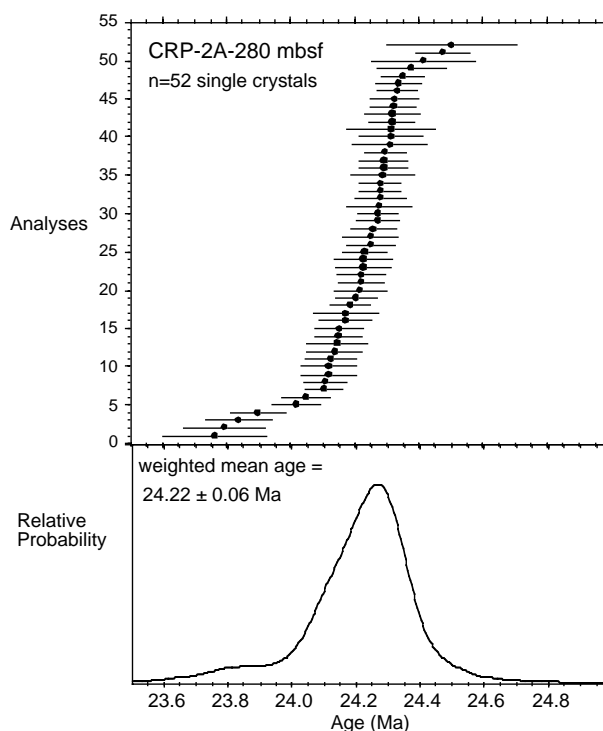


Fig. 7.2 - Probability distribution diagram of single-crystal laser-fusion analyses from CRP-2A-280 m feldspars. Upper panel shows individual analyses with ± 1 sigma error bars; lower panel shows cumulative probability distribution curve.

Mexico Geochronology Research Laboratory at New Mexico Institute of Mining and Technology, using procedures similar to those described in McIntosh & Chamberlin (1984). All ages were determined relative to the inter-laboratory standard Fish Canyon Tuff sanidine with an assigned age of 27.84 Ma (Deino & Potts, 1990). After rejecting data from two crystals that gave poor data, ages from 52 crystals form a tight group with a nearly perfect Gaussian probability distribution (Fig. 7.2). The weighted mean age of 24.22 ± 0.06 Ma (2 sigma error) is considered to be an accurate age for the eruption that produced the pumice-rich layer at 280 mbsf. The high concentration of pumice at 280 mbsf and the complete lack of older contaminant feldspar grains indicate that this age accurately represents the depositional age of the sampled horizon.

CLIMATIC AND DEPOSITIONAL HISTORY

The history of growth and decay of the Antarctic ice sheet and its links with climatically-driven global sea-level change were two of the questions that the Cape Roberts Project was designed to address. Sedimentological analysis of the core has shown that it can address these questions, at least in part, at this early stage of data analysis and synthesis. High-resolution lithological description of the core and facies analysis were carried out on a bed-by-bed basis to establish vertical changes in depositional environments, and sequence stratigraphic analysis was

used to establish broader trends related to base level fluctuations through the vertical succession.

The section represented in CRP-2/2A can be rationalized into 12 recurrent lithofacies which are: 1) mudstone, 2) interstratified sandstone and mudstone, 3) poorly sorted (muddy) very fine to coarse sandstone, 4) moderate to well sorted stratified fine sandstone, 5) moderately sorted stratified or massive medium to coarse sandstone, 6) stratified diamictite, 7) massive diamictite, 8) rhythmically interstratified sandstone and siltstone, 9) clast-supported conglomerate, 10) matrix-supported conglomerate, 11) mudstone breccia, and 12) volcanoclastic sediment. These facies are interpreted in terms of deposition in glacimarine and open coastal/shelf environments by a combination of tractional currents, fall-out from suspension, sediment gravity flows, rain-out from floating glacial ice and perhaps deposition and redeposition in subglacial positions (see chapter 3, Facies Analysis section). The facies analysis indicates that, by comparison with modern glacimarine settings, the substantial amount of melt-water associated with the glaciers in Oligocene times declined in the early Miocene. In addition, the range of glacimarine facies represented in CRP-2/2A core reflect high rates of sediment discharge by a variety of glacial processes. Such facies do not occur in the present day polar glacial regime of Victoria Land, and are characteristic of polythermal glaciation under warmer climatic conditions. For example, the early Miocene strata of CRP-2/2A have the same features as those of CRP-1, where the setting is most comparable with that of polythermal glaciers in the sub-Arctic (Powell et al., 1998). However, even the oldest strata cored do not indicate the high meltwater flows associated with temperate glaciation, as found in Alaska and Chile. This assessment is consistent with the sparse terrestrial palynomorph assemblage (see chapter 5).

The marine shelf setting is indicated by a number of facies, including mudstone (Facies 1), which is indicative of hemipelagic sedimentation; sandstone and mudstone (Facies 2), which are indicative of either waves and marine currents or sediment gravity flows; poorly sorted sandstones (Facies 3) which were deposited by sediment gravity flows or settling from turbid plumes; stratified fine sandstones (Facies 4), with possible hummocky cross-stratification, which are indicative of wave-base settings; planar to cross-stratified medium to coarse sandstone (Facies 5), which is indicative of shoreface and delta-front environments; rhythmic sandstones and siltstones (Facies 8), which are interpreted as cyclopsams and cyclopels from highly sediment-charged glacial streams in the sea; and volcanoclastic-rich sediment. Furthermore, the gradational contacts of the diamictites (Facies 6 and 7) and the interbedding of some diamict intervals with other marine facies is indicative of proximal glacimarine redeposition and rain-out processes.

The shallow marine settings appear to have varied from the shoreface to below wave base and included deltaic and/or grounding-line fan settings with large fluvial discharges. These produced glacial facies such as conglomerates, cyclopels and cyclopsams as well as the

associated delta/fan front and prodeltaic/fan sediment gravity flow deposits. The fan setting, and perhaps also the deltaic setting, are associated with ice-contact and ice-proximal environments. Grounding-line fan systems commonly include debris flow diamictites and associated penecontemporaneous sediment deformation. However, the deformation in the sequence may also result from glacial over-riding or local tectonically-induced brecciation and intrusion. Fabric analyses thus far indicate no strong sub-glacial till fabric, but it remains for further analysis to determine if some diamictites were subglacially deposited.

In the overall context of a shallow marine succession, if sub-glacial erosion, over-riding and deposition has occurred, the ice margin must have grounded offshore. The relatively flat shoreface and shelf during phases of glacial retreat may have had relief in the form of morainal banks produced by grounding-line deposits during advance periods. Relief of this type was probably sufficient to produce mass flow and sediment redeposition in the shelf setting. Some macrofossil assemblages and the darker Facies 1 mudstones of distal glacimarine and paraglacial conditions may have formed when isolated banks created restricted circulation conditions on their shoreward margins. Nearby volcanic eruptions contributed volcanic ash of variable composition into the sea, and most of it subsequently was reworked there.

The recognition of vertically-stacked cyclical facies successions bounded by sharp erosion surfaces has allowed the cored interval to be subdivided readily into sequences. It is suggested here that sequence boundaries coincide with glacial surfaces of erosion that record periods of glacier ice advancing across the sea-floor. In many cases, these advances have occurred in concert with sea-level fall. Sequence boundaries may have formed by two processes: (1) direct grounding of glacier ice onto the sea floor, or (2) erosion from debris-flow diamictites spilling off the front of proglacial grounding-line fans. In the latter case, subsequent ice-contact erosion may remove any evidence of the grounding-line fan. The constituent facies assemblage of each sequence has been interpreted as representing an ice-proximal record of glacial advance and retreat followed by a period of relatively ice-free paraglacial or open marine sedimentation. Sequences display a characteristic vertical organisation of lithofacies that have been subdivided into systems tracts, and include the following elements in ascending stratigraphical order (Fig. 7.3):

- 1 - LST-TST: a sharp-based, poorly sorted, coarse-grained unit comprising diamict and/or conglomerate, which is interpreted as ice-proximal and ice-contact glacimarine sedimentation during the advance and retreat of glacier ice into a shallow marine setting;
- 2 - TST: a fining-upwards interval of muddy sandstone which passes up-section into fine sandy mudstone, and is interpreted as the distal marine record of glacier retreat during sea-level rise;
- 3 - HST: a mudstone that passes gradationally upwards into a muddy sandstone/sandstone facies assemblage, which is interpreted as shoaling from mid/outer shelf to inner shelf water depths under a sea-level highstand;

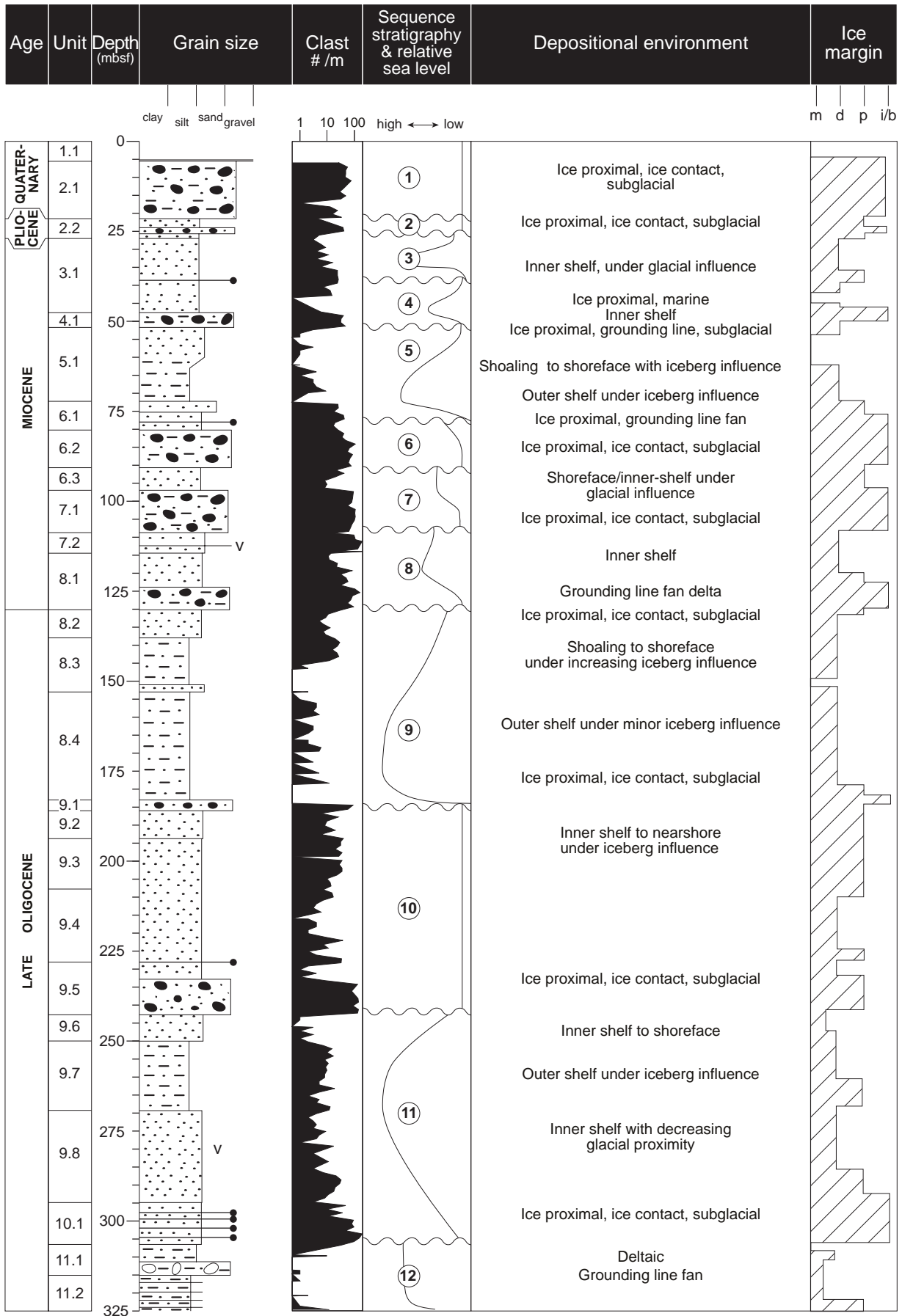


Fig. 7.3 - Stratigraphical summary and interpretation of the CRP-2/2A core.

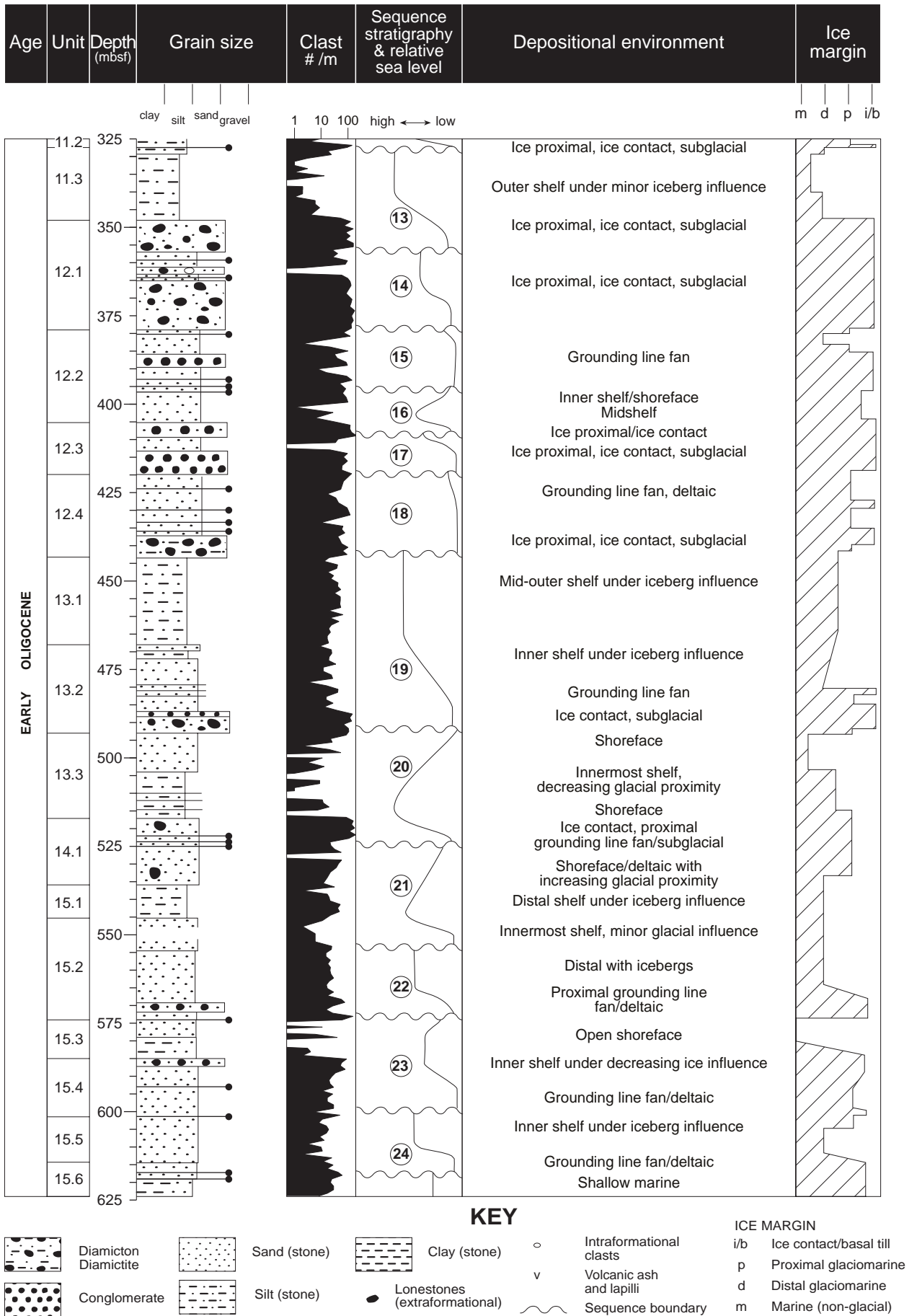


Fig. 7.3 - Continued.

4 - RST: a sharp-based, well-sorted, massive to cross-bedded sandstone, which is interpreted as a regressive facies assemblage forming in a proglacial deltaic depositional environment seaward of the advancing ice front.

Twenty-four cycles of local advance and retreat of glacier ice during the Oligocene to Quaternary can be identified on the basis of the preliminary facies and sequence stratigraphical analysis of the CRP-2/2A core. The Quaternary and Pliocene intervals, Sequences 1 and 2, respectively, are probably an amalgamated series of sequences recording a cryptic and incomplete glacial history of the last 5 Ma. That the Quaternary record lies within a normal polarity interval interpreted as representing Bruhnes Chron suggests that high-amplitude climatic variations characteristic of the last 700 ky may have driven major glacial episodes, destroying much of the earlier Plio-Pleistocene stratigraphical record. The recognition of a thin interval of Pliocene glacial/interglacial stratigraphy in CRP-2/2A is important, as significant fluctuations in the size of the Antarctic ice sheet have been inferred from studies of the on-land "Pliocene" Sirius Formation (Webb & Harwood, 1991; Wilson, 1995). Although punctuated by significant unconformities, the Oligocene-early Miocene section of the core is relatively more complete with 6 sequences preserved in the early Miocene and 16 sequences representing the Oligocene.

Broad constraints on the amplitudes of palaeobathymetric fluctuations reveal cyclical changes in water depth from shoreline-inner shelf to outer shelf water depths, perhaps of 50 to 100 m magnitude. These water depth changes are likely to result from the combined influence of eustasy, local tectonism, and sediment supply factors. The isolation of the eustatic sea-level component from a continental-margin sedimentary succession is inherently difficult to achieve. At this stage it has not been possible to estimate the amplitude of any glacio-eustatic component, but the inferred changes in water depth that are illustrated in figure 7.3 are consistent with the magnitude of eustatic water depth changes inferred for the Oligo-Miocene from seismic records (Haq et al., 1988), and deep ocean oxygen isotope records (Vitor & Anderson, 1998).

A preliminary chronology presented in this volume for CRP-2/2A indicates a thick interval of normal polarity in the late Oligocene which may span up to nine sequences. This implies that individual depositional sequences in certain parts of the core may correspond to Milankovitch orbital frequencies (eccentricity). Such an interpretation has several important implications, notably: (1) that the cored interval contains an incomplete record of the Oligocene-Quaternary of western Ross Sea with large periods of time represented at sequence-bounding unconformities, and (2) where sequences are preserved they may represent an important ice-proximal record of orbital control on the dynamics of the Antarctic ice sheet, which has significant implications for understanding the origin of variations in global eustatic sea-level in late Paleogene and Neogene times.

Alternatively, the frequency of sequence cyclicity may be of a longer duration, similar to that of the 3rd order

(0.5-2 Ma) eustatic cyclicity reported on the Haq et al. (1988) sea-level curve, and the composite Cenozoic oxygen isotope curve of Vitor & Anderson (1998). Of importance is that many of the characteristics of this glacial-marine succession can be explained in terms of local glacial processes. Identifying the relative roles of eustasy, tectonism, and local glacial processes on controlling the depositional architecture of this important Antarctic record is one of the future challenges facing the Cape Roberts Team.

VOLCANIC AND TECTONIC HISTORY

VOLCANISM

Volcanic-derived clasts and grains occur throughout the entire CRP-2/2A core. Reworked basalt fragments are particularly common below 310 mbsf, but their mineralogy and textural characteristics indicate that they were derived by weathering from the Jurassic Kirkpatrick basalt. Evidence for active coeval volcanism is restricted to depths above 469 mbsf, which indicates that volcanism was active in Early Oligocene times, at least, and confirms a history of volcanism in the McMurdo Volcanic Group that is longer than that currently exposed onshore (less than 19 My; Kyle, 1990; *cf.* George, 1989). Volcanic glass occurs only in trace amounts up to 280 mbsf, where a layer of evolved pumice lapilli marks the base of a volcanic-rich interval that continues up to 200 mbsf. This indicates a significant period of volcanism during the Late Oligocene. A second volcanic-rich interval is present between 150 and 46 mbsf, marking a Late Oligocene/Early Miocene episode, and a third (Pliocene) episode is recorded in LSU 2.2 (21.1-26.8 mbsf). The volcanism was bimodal (basaltic/?trachytic) in each case and was probably alkaline, which is characteristic of continental rift settings. The glass was probably derived mainly by rapid reworking from local sources and was deposited by sedimentary rather than pyroclastic processes, and therefore does not provide a complete record of volcanic activity in the region (*cf.* Cape Roberts Science Team, 1998).

Evolved (trachytic?) pumice lapilli are common in LSU 7.1 and 7.2 (*c.* 97-114 mbsf), and LSU 7.2 includes a prominent trachytic tephra layer 1.2 m thick. The thickness and coarse grain-size of the 1.2 m-thick tephra layer indicates derivation from a volcano possibly situated only a few tens of km from the CRP-2/2A drill site. This is consistent with the interpretation of a local source for the glass in the associated sediments. Possible locations of the Oligocene/Lower Miocene volcanic source(s) are uncertain, but may include two small, but prominent, magnetic anomalies of likely volcanic origin identified *c.* 6 km west of CRP-2/2A, and larger anomalies situated *c.* 12 km to the northwest, near Granite Harbour (called the 'Barrett anomaly'), and *c.* 80 km to the ENE (the 'Kyle anomaly') (Behrendt et al., 1987; Behrendt, 1990). The origin of the 1.2 m-thick tephra deposit in LSU 7.2 is uncertain. Whilst deposition by air fall and settling through water are possible, other origins, including secondary thickening and redeposition are being tested.

PROVENANCE AND TRANSANTARCTIC MOUNTAINS UPLIFT

The clast and sand grain assemblages can be divided into three contrasting types: an upper assemblage (0 to 280 mbsf) with a multi-component source (granitoids, sediments, dolerite and abundant contemporary volcanic detritus), a middle assemblage (280-310 mbsf) which is similar to the upper assemblage but essentially lacking a volcanic component, and a lower assemblage (*c.* 310-625 mbsf) which contains numerous fine-grained Jurassic dolerite and basalt fragments and (?)Beacon sedimentary detritus, and in which the proportion of granitoids diminishes markedly toward the base (Fig. 7.4; and see chapter 4, Basement Clasts). In addition, below *c.* 310 mbsf, hornblende and biotite, which are common granitoid minerals, become scarce, reworked Jurassic basalts become abundant, and there is a significant increase in the proportion of Beacon-derived coal debris and rounded quartz grains. This is also reflected (from *c.* 350 mbsf) in lower feldspar/quartz ratios in the sediments. Thus, 310 mbsf marks a major petrological transition which represents a fundamental change in provenance, reflecting an upward change from detritus derived predominantly from Jurassic dolerites, lavas and Beacon sedimentary rocks, to detritus containing additional abundant basement granitoid material.

The provenance change records erosion down through the Beacon Supergroup and Ferrar Group sequence above the Kukri Erosion Surface to expose the sub-Kukri basement complex. This may represent progressive uplift of the Transantarctic Mountains (the likely provenance) or it may be climate-related. Other features in nearby levels of the CRP-2/2A core, including an unconformity at *c.* 307 mbsf, a thick intraformational breccia at 311 to 315 mbsf, and a possible change in stratal dip at *c.* 296 mbsf, are possibly attributable to tectonism and could be interpreted as an indication of faulting that affected the basin margin. If these features prove to be of tectonic origin, the change in provenance may coincide with an episode of faulting and uplift in the Transantarctic Mountains beginning at *c.* 30 Ma.

DEFORMATION

Brecciation, soft-sediment deformation (folding, convolute bedding, shear zones) and sedimentary dykes are common in the CRP-2/2A core. It is clear that more than one phase of deformation occurred, and these phases may reflect glacetectonic, mass movement, and/or tectonic activity (see chapter 3, Deformation section). An intraformational breccia between *c.* 311 and 315 mbsf contains angular to subrounded clasts and possibly resulted from slope failure, perhaps in response to tectonic instability within the basin. Microfaults and sedimentary intrusions are also abundant in the interval from *c.* 309 to 325 mbsf, which could be another indicator of tectonic instability. There is an intriguing association of these features with an unconformity at *c.* 307 mbsf, which is inferred to mark the Early to Late Oligocene boundary, and an interpreted angular discordance in seismic reflectors at *c.* 296 mbsf.

Brittle fractures, abundant throughout CRP-2/2A, are consistent with the structural setting of the site in proximity to the Transantarctic Mountains - Victoria Land Basin boundary. Natural fracture types include brittle microfaults, veins and clastic dykes. Most faults, including sediment- and vein-filled varieties, have normal-sense offset of bedding and in some cases have clear conjugate fault geometry. The geometry and kinematics of these fault arrays is characteristic of a rift environment and most likely records rift-related tectonic deformation in the Cape Roberts area. When fault orientation patterns can be determined from oriented core, it will be possible to compare the trends of faults in the core with seismically mapped faults in the Cape Roberts area to help to constrain the timing and kinematics of regional faulting. Drilling-induced and coring-induced fractures are also abundant in CRP-2/2A core, and preliminary analysis of oriented borehole televiewer imagery of the borehole walls suggests that there may be a consistent northeast-southwest orientation of the steeply-dipping induced fractures. If borne out by detailed analysis, this would indicate that the contemporary maximum horizontal compressive stress has a NE-SW orientation, oblique to the Transantarctic Mountains Front.

BASIN HISTORY

The pre-Pliocene strata of CRP-2/2A span the time interval from *c.* 19 to 33 Ma and accumulated at an average rate of 100 m/My. Subsidence along the margin of the Victoria Land Basin must have accommodated this substantial accumulation of Miocene and Oligocene strata. Sequence stratigraphical analysis has revealed cycles with marked thickness changes and, if the timing of the cycles is relatively uniform, this may reflect tectonically-driven changes in basin subsidence rate and/or sediment supply from the Transantarctic Mountains. An upward change from relatively thin to thick cycles occurs across the inferred Early to Late Oligocene unconformity at *c.* 307 mbsf (28-30 Ma), which possibly marks an increased subsidence rate. There is a change from thick to thinner cycles across an Early Oligocene unconformity at *c.* 443 mbsf, which possibly indicates a decreased subsidence rate in that part of the record.

CRP-2/2A results provide new age constraints for seismic reflectors in the Victoria Land Basin. There are two possible alternatives for the major V3/V4 seismic boundary, at *c.* 80 and 183 mbsf with *c.* 21 Ma (Early Miocene) and 26-27 Ma (Late Oligocene) ages, respectively. Additional reflectors in the sequence are all of Oligocene age. Because these reflectors can be tied to the regional seismic stratigraphy of the Victoria Land Basin, these new age data will provide a means to improve our understanding of the evolution of the Victoria Land Basin and the timing of rift episodes that shaped it.

Velocity data measured from CRP-2/2A core (see chapter 2, Core Physical Properties section) show relatively high seismic velocities for the sedimentary section. Conversion of seismic travel times to depth using the physical properties data yields higher dips for the seismic

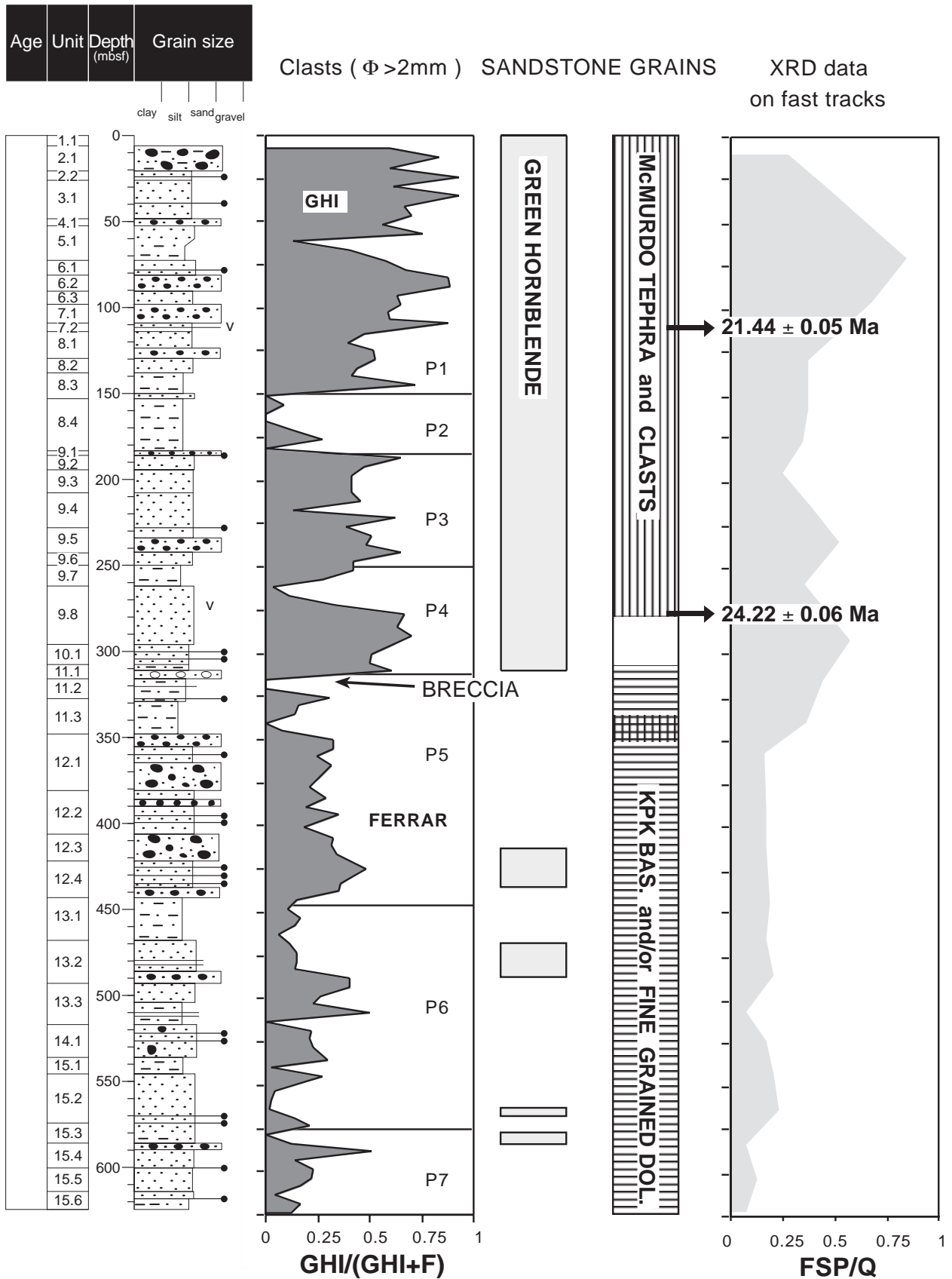


Fig. 7.4 - Summary diagram showing major petrological changes in the CRP2/2A sequence. GHI: Granite Harbour Intrusives; F: Ferrar; KPK BAS.: Kirkpatrick basalt; DOL.: dolerite.

reflectors than was previously interpreted (see Fig. 1.4). Reflector dips define a fan between *c.* 183 mbsf (possibly the V3/V4 boundary) and the major reflector at *c.* 296 mbsf. Dips beneath the reflector at *c.* 296 mbsf steepen from *c.* 5

to 10°. The relatively steep dips are maintained below this depth, including the V4/V5 boundary. The increase in dip documents basinward tilting of the strata. If the fan-shaped arrangement of the reflectors is real, it indicates a

gradual increase in the tilt of older strata through the sequence. If an angular unconformity is present, this suggests distinct phases of tilting that may document discrete rift episodes. More detailed analysis of seismic dips and possible onlap and/or downlap relations of the reflectors may constrain the timing of episodes of tilting, and therefore of faulting events, that affected the basin margin.

When correlations in age, lithostratigraphy, physical properties, and provenance trends are established between CRP-2/2A and CIROS-1, it will be possible to evaluate key issues regarding the tectonic evolution of the Transantarctic Mountains and Victoria Land Basin in the McMurdo Sound area. Detailed comparison of provenance history may reveal either regionally consistent uplift patterns or different uplift histories for discrete crustal blocks along the range, *i.e.* for the Convoy Range, McMurdo Dry Valleys and Royal Society Range blocks, which are divided by structures lying along or close to Mackay Glacier and Ferrar Glacier, respectively (Fitzgerald, 1992; Fitzgerald & Baldwin, 1997). Comparison of age, thickness, and dips of lithostratigraphical sequences between CRP-2/2A and CIROS-1, as well as correlation of seismic reflectors parallel and transverse to the coastline, will constrain models for the subsidence history of the Victoria Land Basin margin and its relationship to faulting along the Transantarctic Mountains Front.

CONCLUSIONS AND FUTURE PLANS

Drilling at CRP-2/2A has yielded more or less continuous core recovery (95%) through about 600 m of strata that have recorded climatic and tectonic history on the margin of the Victoria Land Basin from *c.* 19 to *c.* 33 Ma. The strata have proved to be significantly younger than expected, and cover about the same time interval as the CIROS-1 drill hole 70 km to the south. While this has meant further delay in sampling strata representing earlier climatic and tectonic events, two features give CRP-2/2A special significance in advancing the main goals of the project through offering the prospect of a dramatic improvement in dating strata on the Antarctic continental shelf.

The first feature is the biota being recovered from the core. Although some facies are unproductive, many have well-preserved assemblages, notably of diatoms and marine palynomorphs, some of which include taxa not yet described. These assemblages show progressive changes through the sequence that can provide the basis for a much better circum-Antarctic biostratigraphy. For reasons that we do not understand, the microfossil assemblages in CRP-2/2A are significantly more varied and better preserved than in CIROS-1.

The second feature is the occurrence of volcanic debris and shell fragments throughout most of the core. These materials provide a way of dating a number of stratigraphical levels independent of each other and of the few biostratigraphical datums that can be recognized from lower latitude taxa. The most striking is the volcanic ash layer at 112 mbsf, for which an age of 21.44 ± 0.05 Ma has

already been obtained (see chapter 4, Volcanic Clasts section). A further ash at 280 mbsf has been sampled for dating, and has provided another reference point for building a chronology for the Cape Roberts sequence. A number of volcanic clasts have also been collected in order to provide maximum ages for the levels from which they have been sampled.

The volcanic material extends down only to 469 mbsf, but shell fragments, from which ages can be estimated from the isotopic composition of strontium, were found throughout the length of the core. Although the accuracy of this approach is an order of magnitude lower (0.5 Ma vs 0.05 Ma), the wider distribution of the material will make the results from this work invaluable. In addition to these features, the intensive palaeomagnetic measurements carried out on the full length of the core are providing a reversal stratigraphy that, once calibrated, will enhance further the chronology for CRP-2/2A. When this has been integrated with the biostratigraphical datums yet to be established from the assemblages now being described for the first time, biostratigraphical schemes comparable with that of middle and low latitudes should be achievable for correlation of shelf sequences around the Antarctic margin and into lower latitudes.

One of the main goals of the project is to seek a record of climate and sea level from the climatically sensitive Antarctic margin. Preliminary assessment of the sequence cored in CRP-2/2A indicates that the sequence is entirely marine, but varies from nearshore to offshore, with sedimentation keeping pace with subsidence over the 14 million years spanned by the core. The preliminary age model also suggests two significant gaps in the record, from 21 to 26 Ma and from 28 to 30 Ma, but, of the strata preserved, 22 depositional sequences are recognized, each representing part of a cycle of glacial advance and retreat, and, in some cases, associated with falling and rising sea level. The cycles vary in thickness and time span but average *c.* 30 m and 300 000 years. Features in the core indicate that the climate was much warmer than today and perhaps comparable with that of the margins of the Quaternary ice sheets in the Northern Hemisphere. If the preliminary chronology is accurate, then this suggests that the Antarctic ice sheet in a warmer climatic regime may have a naturally longer period than the northern ice sheets of the Quaternary with their 40 and 100 ka cycles. A significant opportunity that the core is providing is for the analysis of various properties for cyclicity with the three main Milankovitch frequencies. Early results suggest that there are cyclicities on Milankovitch frequencies, but that these are much shorter than the cycles of ice advance and retreat.

The other principal goal of the project, to elucidate the early tectonic history of the Victoria Land Basin and the adjacent Transantarctic Mountains, has also been advanced significantly with the record of progressive erosion through the mountains being recorded in the clasts and minerals in the core. The shift from Beacon and Ferrar rocks, including Kirkpatrick basalt, which caps the Beacon Supergroup at the head of the Mackay Glacier 100 km from the coast, in the lower part of the core, to largely basement-derived clasts above 300 mbsf, plainly records the stripping of the

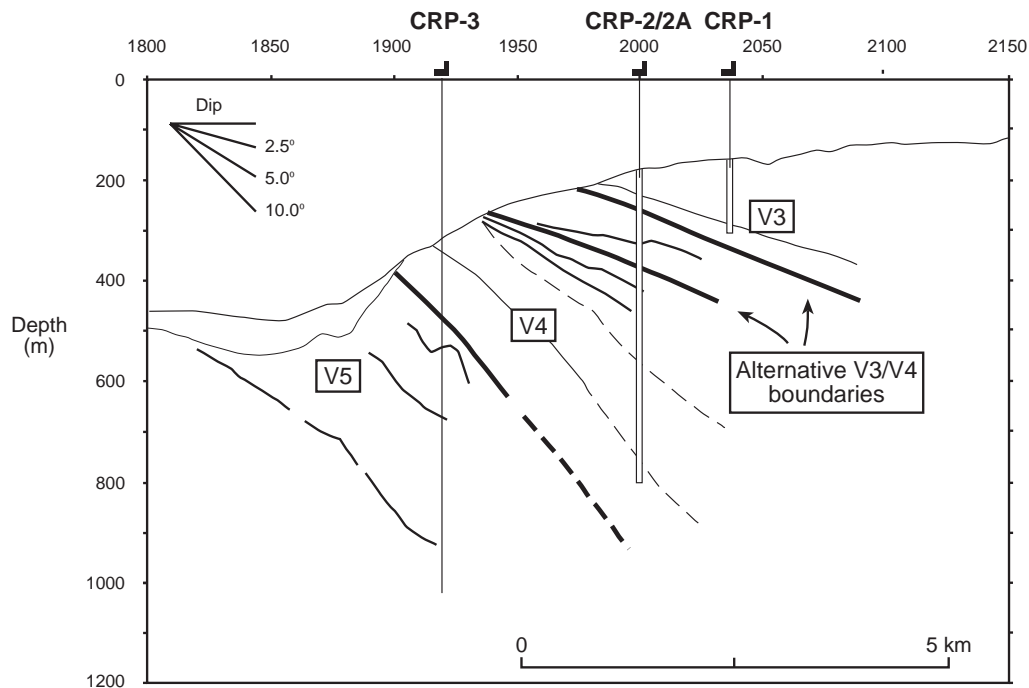


Fig. 7.5 - Depth section from seismic line NBP9601-89, showing the location for CRP-3 in the next drilling season.

landscape through the Devonian-Jurassic “cover beds”. Whether this represents contemporaneous middle Cenozoic uplift, or erosion responding to an earlier rapid uplift event is not yet clear. Work on old and new fracture patterns in the core will yield results for a Neogene stress history for the area. Whatever the changes in stress regime, however, the slow subsidence at this point of the margin of the Victoria Land Basin (around 40 m/Ma net) suggests that the margin of the West Antarctic Rift System has not been tectonically very active in Neogene times.

The drilling in 1998 has completed coring of a little over half of the 1 200 m of strata that were originally targeted, though we have yet to reach strata old enough to record the changes in climate and tectonics in the region that are the primary target of the project. The age of the oldest strata cored this year takes us close to the widely accepted transition period, from *c.* 36 to 34 Ma, from “green-house” to “ice-house”. In the next and final drilling season, we expect to core down through this period.

CRP-3 will be sited to core the lower 50 m of CRP-2A to ensure that the two cored sequences can be linked precisely by correlation using a range of techniques, including down-hole logging, core properties,

lithostratigraphy and biostratigraphy. Water depth at the site will be a little over 300 m and the target depth will be 700 mbsf. This will take us deep into seismic sequence V5, which lies just 120 m below the bottom of CRP-2/2A and the oldest sequence in the Victoria Land Basin (Fig. 7.5).

Some aspects of the drilling operation in 1999 will be easier and others will be more difficult. The experience this year with the new sea riser should help speed the deployment process, and coring through older and harder strata should make for few drilling problems. However, the riser will be set in much deeper water, and there will undoubtedly be fresh problems to be overcome.

Drilling supplies have already been ordered for shipment to Antarctica in January 1999, in preparation for transporting by sledge to Cape Roberts in the early spring. We are hoping that ice conditions will allow us to proceed as planned, and this will be evident from satellite imagery in June 1999. If conditions are marginal, then drilling will be postponed a further season. In the meantime, the focus for the Cape Roberts Science Team is on the more than 5 000 samples and 600 m of logs to be studied for contributions to the Scientific Results volume, due for the workshop in Wellington on 28 June 1999.